



Comparison of Young's Modulus determination from Ultrasonic Testing and Three-Point Bending Testing

Asa Fansuri Abu Samah¹, Rafidah Hasan^{1,2,*}, Zurina Shamsudin²

¹ Fakulti Teknologi dan Kejuruteraan Mekanikal, Universiti Teknikal Malaysia Melaka, Hang Tuah Jaya, 76100 Durian Tunggal, Melaka, Malaysia

² Centre for Advanced Research on Energy, Universiti Teknikal Malaysia Melaka, Hang Tuah Jaya, 76100 Durian Tunggal, Melaka, Malaysia

ARTICLE INFO

Article history:

Received 12 April 2024

Received in revised form 6 June 2024

Accepted 19 June 2024

Available online 30 July 2024

Keywords:

Young's Modulus, Mechanical Testing, 3D printing, Stainless Steel 316

ABSTRACT

This study investigates the comparison of Young's modulus value from ultrasonic testing and three-point bending testing. Three specimens from SLM stainless steel 316 were created using Emarksan Enavision 120 with process parameters of 248.84 W laser power, 1000 mm/s scanning speed, 0.1 mm hatch distance, and 0.04 layer thickness, 62.21 J/mm³ energy density, and stripe scanning strategies with 67° scanning rotation. Three specimens from stainless steel 316 were fabricated from conventional plate using waterjet cutting machine. Ultrasonic tests were done on each sample from SLM stainless steel 316 and stainless steel 316 by following ASTM A578. The three-point bending experiments of SLM stainless steel 316, and stainless steel 316 specimens were following ASTM D790, and ASTM E290, respectively. Ultrasonic testing and three-point bending testing were done on both materials to find the Young's Modulus values. The results obtained from both experiments were compared to each other as well as to standard value. The results show that Young's modulus values from ultrasonic testing are more comparable to the standard value than that from three-point bending testing. These are due to high stress concentration on three-point bending test, which have some effect on Young's Modulus values.

1. Introduction

Young's modulus is fundamental parameter that describes the stiffness of elastic material, and it can be expressed mathematically as ratio of stress divided by strain [1,2]. It is essential to determine Young's modulus of material before applying expected loads on it. Both destructive testing (DT) and non-destructive testing (NDT) can be used to determine material's Young's Modulus.

Destructive test (DT) is conventional method to evaluate material stiffness by applying force on specific place to break down particular material. The most commonly performed destructive tests are tensile, bending, impact, shear, and compression with open and closed holes. Different testing methods can be applied to calculate mechanical properties including stress and Young's Modulus. In most cases, it is recommended to use three-point bend and tensile test methods when determining

* Corresponding author.

E-mail address: rafidahhasan@utem.edu.my

<https://doi.org/10.37934/aram.121.1.5865>

Young's Modulus of materials [2]. There were studies using three-point bending testing that determined flexural behaviour of Engineered Cementitious Composite (ECC) and mechanical properties of alloy wires. Wee *et al.*, [3] studied on two different contents of ECC mixtures flexural behaviour, and Dechkunakorn [4] studied on superelastic nickel-titanium alloy wires from different manufacturers to investigate mechanical properties for appropriate selection in orthodontic treatment.

Non-destructive testing (NDT) methods mostly depend on the measurement of propagation speed through the application of acoustic or ultrasonic waves, which allows to calculate the Young's Modulus. Also, non-destructive tests like ultrasonic test does not break and damage material. Tested material from non-destructive test remains unchanged like as-received condition. There were studies using ultrasonic testing that determined the mechanical properties of polymer composites and metals. Oral *et al.*, [5] conducted study on epoxy resin for measurement of mechanical properties of polymer composites for different ratios and Ediguer *et al.* [6] studied on 304 stainless steel with 3.1 % numerical error measurement of mechanical properties. The experiment showed that the application of ultrasonic testing can evaluate the mechanical properties of both polymer composites and metals.

From literature review, there is not much comparison between two testing methods (ultrasonic testing and three-point bending testing) to determine Young's modulus value and similarities between two methods. This study is to compare Young's Modulus determination from ultrasonic test and three-point bending test.

2. Methodology

2.1 Materials

In this study, Selective Laser Melting (SLM) stainless steel 316 and standard conventional stainless steel 316 were used as material testing for ultrasonic testing and three-point bending testing to determine Young's Modulus. SLM stainless steel 316 specimens were fabricated using Ermaksan Enavision 120 SLM machine. Spherical Ermak S 316 L-A11 powder was used as feedstock for fabrication and range of particle metallic powder is 15-45 μm . The process parameters of SLM is 248.84 W laser power, 1000 mm/s scanning speed, 0.1 mm hatch distance, and 0.04 layer thickness, 62.21 J/mm³ energy density, and stripe scanning strategies with 67° scanning rotation. Meanwhile, standard conventional stainless Steel 316 specimens were prepared from conventional plate using Flow Mach 2 waterjet cutting machine. SLM stainless steel 316 and standard stainless steel 316 specimens were rectangular with dimensions 100 mm length, 20 mm width, and 5 mm thickness. In total, six specimens were fabricated including three SLM stainless steel 316 specimens, and three stainless steel 316 specimens for ultrasonic test and three-point bending test.

2.2 Density Measurement

SLM stainless steel 316 and standard conventional stainless steel 316 specimens was tested with Electronic Densimeter MDS-300 for measuring density. All measurements were conducted with water at room temperature, which is approximately 25°C. For determining density of specimen, total three readings of density were obtained on every specimen, and average density value was determined. For theoretical value of density, Archimedes method was used to calculate specimen density. Measured specimen's density is given in Eq. (1), where ρ is density of specimen, M_a is measured mass of specimens, measured in air, M_w is measured mass of specimens measured in water, and ρ_w is the density of water.

$$\rho = \left(\frac{M_a}{M_a - M_w} \right) \rho_w \quad (1)$$

2.3 Surface Roughness Measurement

Surface roughness was tested with non-contact 3D Surface Profilometer Shodensha GR3400. Magnification of this instrument was 10× with Carl Zeiss microscope lens. Readings were obtained at three different positions (left position, center position, and right position) on top surface of SLM stainless steel 316 and standard conventional stainless steel 316 specimens. WinRoof software was used for measuring surface roughness. Total of three readings of surface roughness profile were determined for every specimen, and average surface roughness value (Ra) was determined.

2.4 Preparation of Ultrasonic Testing

Young's modulus value from ultrasonic test was determined according to ASTM A578 (Standard Specification for Straight-Beam Ultrasonic Examination of Rolled Steel Plates for Special Applications) [7]. Olympus EPOCH 650 ultrasonic flaw detector was used to perform straight-beam ultrasonic testing by using Pulse-Echo testing method. Single transducer DL4R-3.5×10 connected to ultrasonic flaw detector for sending and receiving ultrasonic waves and Sonotech Ultragel II as couplant for ultrasonic test. Ultrasonic waves pass through SLM stainless steel 316 and standard conventional stainless steel 316 specimens during application from surface using transducer as shown in Figure 1.

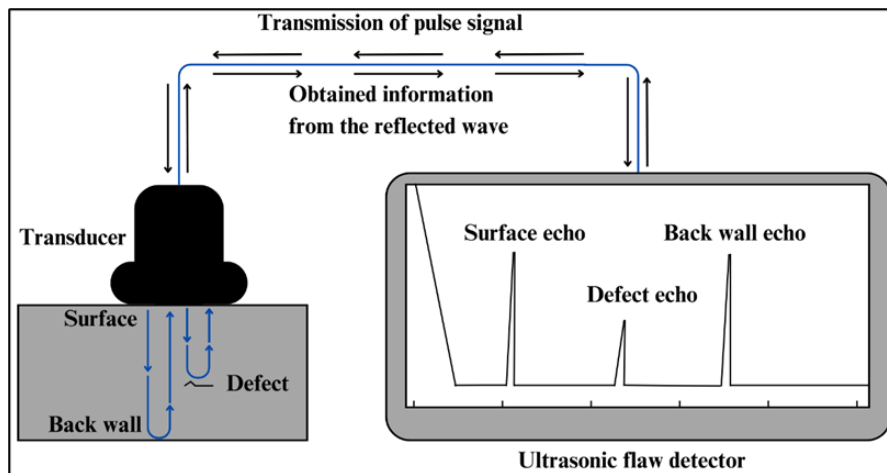


Fig. 1. Schematic diagram of Ultrasonic waves pass through material from surface using ultrasonic transducer testing. This figure was adapted from Ramos et al. (2015)

Calibration of ultrasonic flaw detector were done by applying on calibration block prior to experiments. Calibration of ultrasonic flaw detector must be done to verify the precision of the test results and ensure the proper functioning of the ultrasonic flaw detector. Data were recorded and calculated using sound velocity formula [8] in Eq. (3) that has been simplified from Eq. (2) to determine Young's Modulus where longitudinal waves V_L (m/s), material density, ρ (kg/m³), Young's Modulus E (GPa), and Poisson's ratio ν [9,10]. Poisson's ratio of stainless steel 316 are taken from literature, which value of Poisson's ratio of stainless steel is 0.27 [11].

$$V_L = \sqrt{\frac{E(1-\nu)}{\rho(1-\nu)(1-2\nu)}} \quad (2)$$

$$E = \frac{\rho V_L^2 (1+\nu)(1-2\nu)}{(1-\nu)} \quad (3)$$

2.5 Preparation of Three-point Bending Testing

Young's modulus value from three-point bending test was determined according to ASTM E290 (Standard Test Methods for Bend Testing of Material for Ductility) [12] for stainless steel 316. SLM stainless steel 316 and standard stainless steel 316 specimens were tested using Instron Machine Dynamic Model 5585. Specimens were held by two lower supports, and force of loading pin was applied in the middle of specimens, and deflection appeared after three-point bending test as shown in Figure 2. Distance between two lower supports of SLM stainless steel 316 and standard stainless steel 316 are 80 mm. Experiments were conducted at room temperature. BlueHill Software was used to record raw force-displacement graph from three-point bending tests and it can be transformed to stress-strain graph by using this equation below, where σ is stress in Eq. (4) for rectangular specimen and ε is strain in Eq. (5), where F is Force (kN), L is length of specimens between two lower supports (mm), b is width of specimens (mm), d is thickness of specimens (mm), and δ is deflection at center of specimens (mm):

$$\sigma = \frac{3FL}{2bd^2} \quad (4)$$

$$\varepsilon = \frac{6\delta d}{L^2} \quad (5)$$

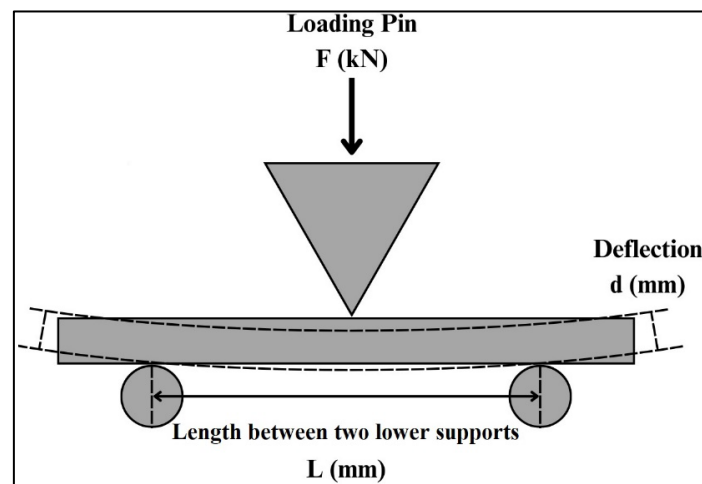


Fig. 2. Schematic diagram of three-point bending test. This figure was adapted from Guseinov et al. (2022)

3. Results and Discussion

3.1 Density of Material

Table 1 shows average density of SLM stainless steel 316, standard conventional stainless steel 316, and previous literature [13] compared to standard stainless steel 316. Standard density value of stainless steel 316 were obtained from Matweb [14]. Average density of standard conventional stainless steel 316 are more comparable with standard density value of stainless steel 316, which

percentage difference is 0.16 %. On the other hand, SLM stainless steel 316 specimen has lower density value compared to standard density value of stainless steel, which percentage difference is 5.88 %. This is due to lack of fusion remaining porosity inside SLM material contribute to density decrease. Metal powders are not fully melted to form new layer on previous layer with sufficient overlap and poor bonding between two layers during solidification process. As a result, porosity increase, and unmelted metal powder remains inside pores in SLM parts [15].

Table 1
 Result of average density of tested specimens

Type of specimen	Average measured density, ρ	Standard density value of stainless steel 316 [14]
SLM stainless steel 316	$7.543 \pm 0.041 \text{ g/cm}^3$	8.0 g/cm^3
Standard conventional stainless steel 316	$7.987 \pm 0.018 \text{ g/cm}^3$	
Bakhtiarian <i>et al.</i> , [13]	7.888 g/cm^3	

3.2 Surface Roughness of Material

Table 2 shows result of surface roughness for tested specimens and other literature. It shows that surface roughness of standard conventional stainless steel 316 specimen has lowest value compared to SLM stainless steel 316 and literature. Meanwhile, SLM stainless steel 316 are comparable to literature, which percentage difference is 3.70 %. According to literature [16], it was stated that SLM machine melt powder partially on surface of SLM parts. As a result, it is does not produce acceptable surface quality. Otherwise, it is also may further effect on mechanical properties of SLM parts. The energy density of SLM influences surface roughness of materials. optimal energy density of SLM leads to melt metal powder completely. Therefore, average surface roughness of SLM parts decrease, due to optimal energy density contribute high melt pool and strong bonds between two particles of materials.

Table 2
 Result of average surface roughness, Ra

Specimen	Average surface roughness, Ra
SLM stainless steel 316	$4.24 \pm 0.93 \text{ }\mu\text{m}$
Standard conventional stainless steel 316	$1.35 \pm 0.16 \text{ }\mu\text{m}$
Jagdale <i>et al.</i> , [9]	$4.40 \pm 1.67 \text{ }\mu\text{m}$

3.3 Sound Velocity of Material

Result of average sound velocity from ultrasonic test as shown in Table 3. Standard sound velocity of stainless steel 316 was obtained from manufacturer datasheet. It shows that standard conventional stainless steel 316 specimen are more comparable average sound velocity compared to standard sound velocity of stainless steel 316 and literature which percentage difference is 6.31 % and 8.28 %, respectively. On the other hand, SLM stainless steel 316 specimen has lower value compared to standard conventional stainless steel 316, which percentage difference of SLM stainless steel 316 compared to standard sound velocity value of stainless steel 316 and literature is 17.23 % and 19.19 %, respectively.

Table 3

Result of average density of tested specimens

Type of specimen	Average sound velocity, V_L	Standard sound velocity value of stainless steel 316
SLM stainless steel 316	4830 m/s	5740.40 m/s
Standard conventional stainless steel 316	5389 m/s	
Khan <i>et al.</i> , [5]	5855 m/s	

It was suggested that wave propagation and reflection of ultrasonic test are influenced by porosity in materials [17]. Porosity in SLM stainless steel 316 cannot be avoided due to influence of SLM processing parameters including laser energy density, laser power, scanning speed, hatch distance, layer thickness, and and strips overlap as shown in Figure 3. It was reported on literature [18], it is stated that porosity leads ultrasonic waves scattered and attenuated due to appearance of lack of fusion in materials, which is ultrasonic waves travel to longer path to cover material thickness, which decreases the sound velocity drastically.

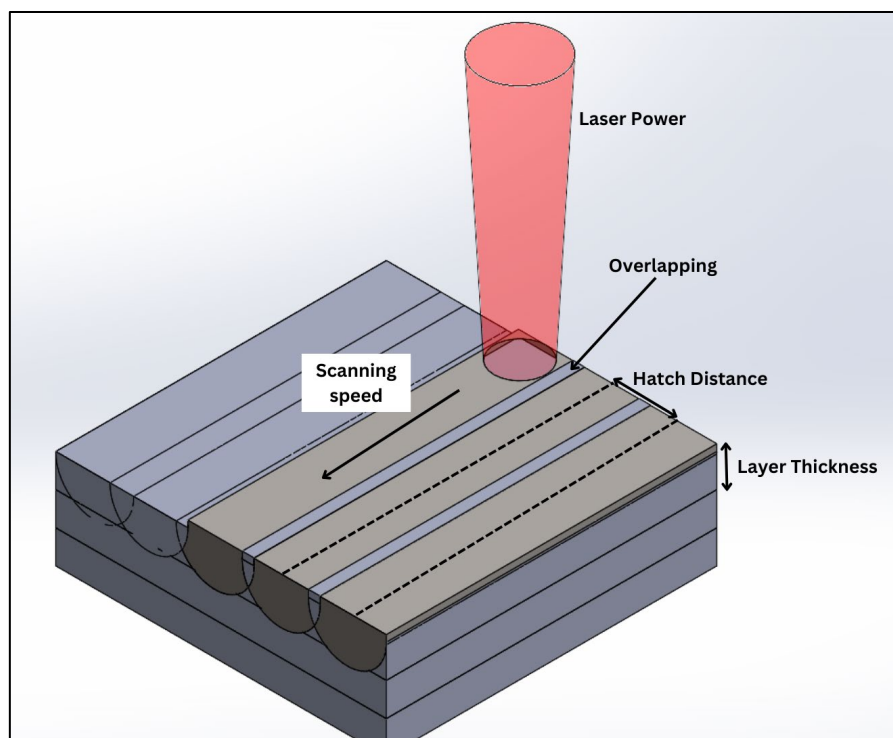


Fig. 3. Schematic diagram of process parameters of SLM during process. This figure was adapted from Yap *et al.* [22].

3.4 Determination of Young's Modulus

Table 4 shows Young's modulus value of SLM stainless steel 316, standard conventional stainless steel 316, and previous literature from ultrasonic test [19], three-point bending test, and standard Young's modulus value of stainless steel 316. Standard Young's modulus value of stainless steel 316 was obtained from Matweb [14]. In ultrasonic testing, it shows that standard conventional stainless steel 316 specimen are more comparable with standard Young's modulus of stainless steel 316, which percentage difference is 6.15 %. On the other hand, Young's modulus value from three-point bending test also shows standard conventional stainless steel 316 is higher than SLM stainless steel

316 and Kozub et al. [20], which percentage difference compared to standard Young's modulus value of stainless steel 316 is 50.73 %.

Table 4
Result of average Young's modulus of tested specimens

Type of specimen	Average Young's modulus		Standard Young's modulus value of stainless steel 316 [14]
	Ultrasonic test	Three-point bending test	
SLM stainless steel 316	137.7106 GPa	93.8053 GPa	193 GPa
Standard conventional stainless steel 316	181.4916 GPa	114.8953 GPa	
Kozub <i>et al.</i> , [20]	-	108 GPa	
Victoria <i>et al.</i> , [19]	209 GPa	-	

Low Young's modulus value of SLM stainless steel 316 from ultrasonic test and three-point bending test compared to standard conventional stainless steel 316 and literature because of high average surface roughness in specimens of SLM stainless steel 316 contribute to high stress concentration [21]. According to literature, it is reported that high surface roughness on SLM parts can be considered as natural micro-notch, where local stress concentration promotes crack initiation and propagation. Surface roughness of as-built SLM parts influences by energy density of SLM. Insufficient. Defects occurred in partially molten particle with powder and created solidified shape of laser scanning track. Micro-cracks and balling effect increase surface roughness of SLM parts. Therefore, High stress concentration on surface leads to decrease mechanical properties of SLM parts.

4. Conclusions

The overall results have been discussed in this paper. It is shows that Young's modulus value from ultrasonic test is higher than Young's modulus value from three-point bending test. It is also shown that standard conventional of stainless steel 316 has higher value in density, sound velocity, surface quality, and Young's modulus compared to SLM stainless steel 316.

From this study, it is shown that more analysis should be done on process parameters of SLM stainless steel 316 where energy density of SLM can be factor that effect on mechanical properties in the future.

Acknowledgement

This study is funded by Ministry of Higher Education (MOHE) of Malaysia through the Fundamental Research Grant Scheme (FRGS), No: FRGS/1/2022/TK10/UTEM/02/20. The Authors also would like to thank Universiti Teknikal Malaysia Melaka (UTeM) for all the supports. This works have initially been accepted and presented at the ICE-SEAM 2023. Also, this paper is full writing of extended abstract of ICE-SEAM 2023.

References

- [1] Ma, Y. Zee, David Sobernheim, and Janz R. Garzon. "Glossary for unconventional oil and gas resource evaluation and development." In *Unconventional oil and gas resources handbook*, pp. 513-526. Gulf Professional Publishing, 2016. <https://doi.org/https://doi.org/10.1016/B978-0-12-802238-2.00019-5>
- [2] Wang, Chenguang, and Changquan Calvin Sun. "A critical examination of three-point bending for determining Young's modulus." *International journal of pharmaceutics* 629 (2022): 122409. <https://doi.org/https://doi.org/10.1016/j.ijpharm.2022>

- [3] Wee, Lee Siong, Mohd Raizamzamani Md Zain, Oh Chai Lian, Nadiyah Saari, and Norrul Azmi Yahya. "Compression and Flexural Behavior of ECC Containing PVA Fibers." *Pertanika, J. Sci. Technol.* 30 (2022): 277-289. <https://doi.org/10.47836/pjst.30.1.15>
- [4] Dechkunakorn, Surachai, Rutchadakorn Isarapatanapong, Niwat Anuwongnukroh, Nattiree Chirananit, Julatthep Kajorchaiyakul, and Anak Khantachawana. "Mechanical properties of several NiTi alloy wires in three-point bending tests." *Applied Mechanics and Materials* 87 (2011): 14-19. <https://doi.org/10.4028/www.scientific.net/amm.87.14>
- [5] Oral, Imran, Hatice Guzel, and Gulnare Ahmetli. "Determining the mechanical properties of epoxy resin (DGEBA) composites by ultrasonic velocity measurement." *Journal of applied polymer science* 127, no. 3 (2013): 1667-1675. <https://doi.org/10.1002/app.37534>
- [6] Ediguer E., Juan M., and Flávio B. "Measurement of elastic properties of materials by the ultrasonic through-transmission technique." *Dyna* 78, no. 168 (2011): 59-64.
- [7] ASTM A578. Specification for Straight-Beam Ultrasonic Examination of Rolled Steel Plates for Special Applications. Philadelphia, PA: ASTM International. 2017. https://doi.org/10.1520/A0578_A0578M-07R12
- [8] Hellier, Charles. *Handbook of nondestructive evaluation*. No. 19496. Mcgraw-hill, 2003. <http://dx.doi.org/10.1036/007139947X>
- [9] Jagdale, Shweta Hanmant, Sumanth Theeda, Bharath Bhushan Ravichander, and Golden Kumar. "Surface morphology and Hardness of powder Bed Fused SS316L as a Function of Process Parameters." *Solid Freeform Fabrication 2022: Proceedings of the 33rd Annual International, Solid Freeform Fabrication Symposium* (2022). <http://dx.doi.org/10.26153/tsw/44546>
- [10] Kumar, Anish, T. Jayakumar, Baldev Raj, and K. K. Ray. "Correlation between ultrasonic shear wave velocity and Poisson's ratio for isotropic solid materials." *Acta materialia* 51, no. 8 (2003): 2417-2426. [https://doi.org/10.1016/S1359-6454\(03\)00054-5](https://doi.org/10.1016/S1359-6454(03)00054-5)
- [11] Ma, Y. Zee, David Sobernheim, and Janz R. Garzon. "Glossary for unconventional oil and gas resource evaluation and development." In *Unconventional oil and gas resources handbook*, pp. 513-526. Gulf Professional Publishing, 2016. <https://doi.org/https://doi.org/10.1016/B978-0-12-802238-2.00019-5>
- [12] ASTM E290. Standard Test Methods for Bend Testing of Material for Ductility. ASTM International: West Conshohocken, PA, USA. 2014. <https://doi.org/10.1520/E0290-14>
- [13] Bakhtiarian, Mohammadamin, Hamid Omidvar, Amirhossein Mashhuriazar, Zainuddin Sajuri, and C. Hakan Gur. "The effects of SLM process parameters on the relative density and hardness of austenitic stainless steel 316L." *Journal of Materials Research and Technology* 29 (2024): 1616-1629. <https://doi.org/10.1016/j.jmrt.2024.01.237>
- [14] Baucchio, Michael, ed. *ASM metals reference book*. ASM international, 1993.
- [15] Zhang, Bi, Yongtao Li, and Qian Bai. "Defect formation mechanisms in selective laser melting: a review." *Chinese Journal of Mechanical Engineering* 30 (2017): 515-527. <https://doi.org/10.1007/s10033-017-0121-5>
- [16] Kaynak, Yusuf, and Ozhan Kitay. "The effect of post-processing operations on surface characteristics of 316L stainless steel produced by selective laser melting." *Additive Manufacturing* 26 (2019): 84-93. <https://doi.org/10.1016/j.addma.2018.12.021>
- [17] Sol, T., S. Hayun, D. Noiman, E. Tiferet, O. Yeheskel, and O. Tevet. "Nondestructive ultrasonic evaluation of additively manufactured AISi10Mg samples." *Additive Manufacturing* 22 (2018): 700-707. <https://doi.org/10.1016/j.addma.2018.06.016>
- [18] Zhang, Chenhao, Bing Chen, HuiMin Li, Xuan Liu, Gaojie Zhou, and Guoqing Gou. "Propagation characteristics of ultrasonic in SLM manufactured AISi10Mg." *Ultrasonics* 135 (2023): 107134. <https://doi.org/10.1016/j.ultras.2023.107134>
- [19] Victoria, B., George, G., Babu, V. "Ultrasonic characterization of austenitic stainless steel in thermal variations." *IJSRSET* 1 no. 6 (2015): 123-126. <https://doi.org/10.32628/IJSRSET151615>
- [20] Kozub, Barbara, Marimuthu Uthayakumar, and Jan Kazior. "The Influence of Nanographite Addition on the Compaction Process and Properties of AISI 316L Sintered Stainless Steel." *Materials* 15, no. 10 (2022): 3629. <https://doi.org/10.3390/ma15103629>
- [21] Renzo, Danilo A., Carmine Maletta, Emanuele Sgambitterra, Franco Furguele, and Filippo Berto. "Surface roughness effect on multiaxial fatigue behavior of additively manufactured Ti6Al4V alloy." *International Journal of Fatigue* 163 (2022): 107022. <https://doi.org/10.1016/j.ijfatigue.2022.107022>
- [22] Yap, Chor Yen, Chee Kai Chua, Zhi Li Dong, Zhong Hong Liu, Dan Qing Zhang, Loong Ee Loh, and Swee Leong Sing. "Review of selective laser melting: Materials and applications." *Applied physics reviews* 2, no. 4 (2015). <https://doi.org/10.1063/1.4935926>